Applied Physics Express **9**, 031202 (2016)
http://doi.org/**10.7567/APEX.9.031202**

Understanding the high p-type conductivity in Cu-excess $CuAlS_2$: A first-principles study

Dan Huang[1,3,4], Yujun Zhao[2], Wenjuan Tang[1], Xianqing Liang[1,3], Wenzheng Zhou[1,3], Changsheng Li[4], Chunmei Yao[4], and Jin Guo[1,3*]

[1]*Guangxi Colleges and Universities Key Laboratory of Novel Energy Materials and Related Technology, College of Physics Science and Technology, Guangxi University, Nanning 530004, China*
[2]*Department of Physics and State Key Laboratory of Luminescent Materials and Devices, South China University of Technology, Guangzhou 510640, China*
[3]*Guangxi Collaborative Innovation Center of Structure and Property for New Energy and Materials, School of Material Science and Engineering, Guilin University of Electronic Technology, Guilin 541004, China*
[4]*Department of Physics and Electronic Sciences, Hunan University of Arts and Science, Changde 415000, China*

*E-mail: guojin@gxu.edu.cn

Received January 12, 2016; accepted February 3, 2016; published online February 22, 2016

The high p-type conductivity in Cu-excess $CuAlS_2$ reported from a recent experimental paper is not well understood as it is not supported by earlier theoretical studies. We found that Cu can be heavily doped at the Al site and can form compensated defect bands to shift up the valence band, leading to shallow acceptor levels under a Cu-excess condition. In particular, Zn doping at the Al site in Cu-excess $CuAlS_2$ has been suggested as a promising approach to improving the p-type conductivity in Cu-excess $CuAlS_2$. © 2016 The Japan Society of Applied Physics

Transparent conductive materials (TCMs) have attracted much attention since they possess the unique combined properties of the transparency of glass and the conductivity of metals.[1,2] The most popular TCMs are all n-type materials, including Sn-doped In_2O_3 (ITO),[3] F-doped SnO_2 (FTO),[4] and Al-doped ZnO (AZO),[5] which are used for front surface electrodes of solar cells and flat-panel displays, low-emissivity windows, touch panel controls, and so forth.[6] The development of functional p–n junctions composed of all TCMs[7] is extremely attractive, since it is expected to open up an era of "invisible electronics".[8] The p-type doping of these commercialized n-type TCMs appears pessimistic despite various attempts.[9] The difficulty in p-type doping in these binary oxides is due to the deep valence band maximum (VBM) dominated by the deep O-2p states,[9] thus leading to the localized holes close to the oxygen atoms and deep acceptor levels.

In 1997, a design principle called "chemical modulation of the valence band" was proposed by Hosono and coworkers.[10] Using the fully filled Cu-3d levels with low binding energy to hybrid with the deep O-2p states, the new compound will possess the VBM from an antibonding state between Cu-3d and O-2p states and thus has a much higher valence band to favor the p-type conductivity. They firstly reported[10] that the delafossite structure $CuAlO_2$ film possessed a conductivity of 1.0 $S \cdot cm^{-1}$ at room temperature. Following that study, other Cu-based delafossite-type oxides such as $CuBO_2$,[11] $CuScO_2$,[12] and $CuCrO_2$[13] were reported to have p-type conductivity. However, their conductivities are still 3–4 orders lower than those of well-established n-type TCMs.

Cu-based sulfides with a suitable band gap, such as $CuAlS_2$[14–23] and $BaCu_2S_2$,[24,25] have also been studied as TCMs, since the valence states of sulfur are higher than that of oxygen. A number of experimental and theoretical works[14–23] have focused on the nonstoichiometric or element-doped $CuAlS_2$ as a promising TCM. Through extrinsic Mg and Zn doping at Al, p-type conductivities have reached 41.7 and 65.3 $S \cdot cm^{-1}$ in $CuAl_{0.94}Mg_{0.06}S_2$[16] and $CuAl_{0.9}Zn_{0.1}S_2$[17] samples, respectively. The highest p-type conductivity[14] with 247.5 $S \cdot cm^{-1}$ among all reported $CuAlS_2$-based TCMs has been achieved in $Cu_{1.08}Al_{0.92}S_2$, which is even higher than the highest p-type conductivity (i.e., 220 $S \cdot cm^{-1}$ in the $CuCr_{0.95}Mg_{0.05}O_2$ sample[13]) among all the p-type delafossite TCMs. On the other hand, on the basis of the theoretical calculations of various defects[20–22] in $CuAlS_2$, the p-type defects V_{Cu}, Cu_{Al}, Mg_{Al}, and Zn_{Al} can have low formation energies and should be the dominant defects under certain growth conditions. The high p-type conductivity in $Cu_{1.08}Al_{0.92}S_2$, however, is still a puzzle as Cu_{Al} was reported to have a deep transition level.[20–22]

In this work, we have studied the electronic structure and defects in Cu-excess $CuAlS_2$ systems by first-principles calculations. Our results show that the valence band shifts up with increasing Cu content owing to the contribution of Cu-3d states to the VBM, coupled with the decrease in Cu–S bond length. Under the Cu-excess condition, the acceptor transition level $\varepsilon(0/-)$ of Cu_{Al}^0 can decrease from 0.44 to 0.14 eV, which markedly improves the conductivity of the $CuAlS_2$ system. In addition, we suggest that Zn doping at the Al site in Cu-excess $CuAlS_2$ samples is a promising approach to increasing further the p-type conductivity.

Our first-principles calculations have been carried out on the basis of the density functional theory (DFT) as implemented in the Vienna ab initio simulation package (VASP).[26,27] The Perdew–Burke–Ernzerhof gradient-corrected functional[28] is used with corrections for on-site Coulomb interactions for strongly correlated systems. Generalized gradient approximation typically underestimates the correlation of localized orbitals of 3d transition metals, and the Hubbard U modification provides an approximate correction for this shortcoming. The values of U_{eff} employed for the Cu-3d and Zn-3d states are 5.2 and 6.5 eV, respectively, which are consistent with the values determined in previous studies.[29,30] To describe the interactions between the valence electrons and the core, the projector augmented wave implementation[31] was used. The energy cutoff of 550 eV was used for all the calculations. For the $CuAlS_2$ unit cell, the special k-point sampling over an $8 \times 8 \times 4$ Monkhorst–Pack mesh[32] was used. $CuAlS_2$ has a chalcopyrite structure (space group number: 122), which is analogous to a zinc-blende structure with its cations substituted by two types of cations alter-

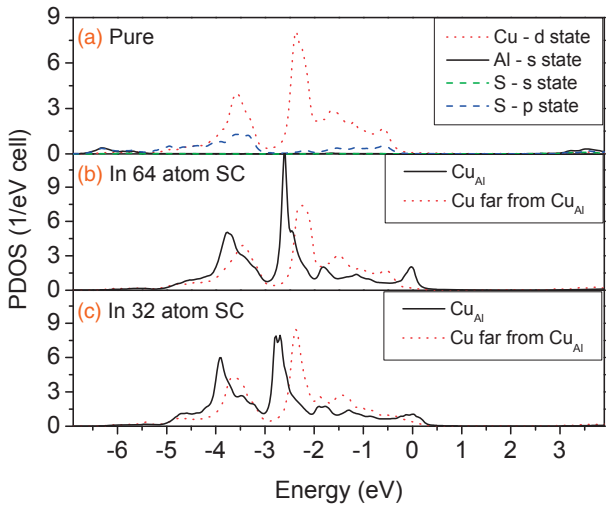

Fig. 1. Partial densities of states (PDOSs) of Cu-3d, Al-3s, and S-3p,4s in $CuAlS_2$ (a) and the PDOSs of Cu-3d of the Cu_{Al}^0 defect and Cu atom in one Cu_{Al}^0 in $CuAlS_2$ 64-atom (b) and 32-atom (c) supercells.

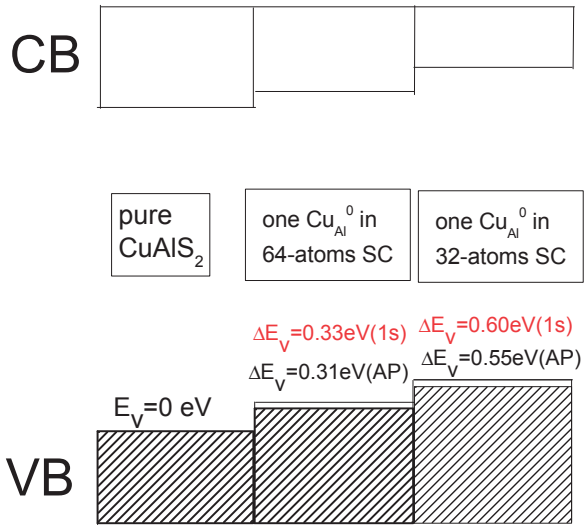

Fig. 2. Band offset among pure $CuAlS_2$, one Cu_{Al}^0 in a 64-atom supercell (SC), and one Cu_{Al}^0 in a 32-atom supercell. With increasing Cu_{Al}^0 concentration, the valence band shifts up. The calculated valence band position changes (ΔE_v) are 0.31 and 0.55 eV [adopted average potentials (APs) as reference energies] and 0.33 and 0.60 eV [adopted core state eigenvalues of 1s orbital (1s) as reference energies] when different reference energies are chosen.

natively along the [001] direction. Our calculated lattice parameters and the anion displacement parameter of $CuAlS_2$ are $a = b = 5.362$ Å, $c = 10.526$ Å, and $u = 0.259$, in good agreement with the experimental measurements $a = b = 5.334$ Å, $c = 10.444$ Å,[33] and $u = 0.268$.[34] Our calculated lengths of Cu–S and Al–S bonds are 2.336 and 2.277 Å, respectively.

For the calculations of defect systems, $\sqrt{2} \times \sqrt{2} \times 1$ supercells containing 32 atoms and $2 \times 2 \times 1$ supercells containing 64 atoms are used. Here, we point out that the $Cu_{1+x}Al_{1-x}S_2$ samples can maintain the chalcopyrite structure under the variation x up to ~10%,[14] which corresponds to our supercells in the calculations. Owing to the heavy doping concentration in the systems, all the supercell parameters including the lattice constants and internal coordinates are fully relaxed throughout this work. The k-point meshes of $6 \times 6 \times 4$ and $4 \times 4 \times 4$ are employed for the $\sqrt{2} \times \sqrt{2} \times 1$ and $2 \times 2 \times 1$ supercells, respectively.

Generally, the VBMs of the Cu-based chalcopyrite compounds Cu–III–VI_2 (III = Al, Ga, In, VI = S, Se, Te) come from the antibonding state of the Cu–VI bond. One reason for this is that the fully filled Cu-3d state has a low binding energy and results in a high valence band.[35] Figure 1(a) shows the partial densities of states of Cu-3d, Al-3s, and S-3p,4s in pure $CuAlS_2$. The majority of the lower valence bands (i.e., the Cu–S bonding state around −6 to −3 eV with respect to the Fermi level) are dominated by Cu-3d and S-3p, and the majority of the upper valence bands (i.e., the Cu–S antibonding state around −3 to −0 eV) are dominated by Cu-3d with a notable contribution from S-3p. Although the chalcopyrite compounds with large defect concentration can maintain their original crystal structure,[14,36,37] the electronic structure may change under a marked composition variation. Figures 1(b) and 1(c) show the partial densities of states of Cu 3d of two different Cu atoms in the Cu_{Al}^0-doped $CuAlS_2$ 64- and 32-atom supercells, respectively. One observes that the Cu-3d level of the defect Cu_{Al}^0 can shift to a much higher energy position compared with the Cu atom far from the Cu_{Al}^0 defect. The bond lengths of Cu_{Al}^0–S are 2.293 Å (64-atom supercell) and 2.289 Å (32-atom supercell), which are clearly smaller than the bond length of Cu–S (i.e., 2.336 Å) in pure $CuAlS_2$. The bond lengths of Cu–S far from the defect Cu_{Al}^0 are 2.330 Å (64-atom supercell) and 2.310 Å (32-atom supercell), which are close to that in pure $CuAlS_2$. Owing to the smaller Cu_{Al}^0–S bond length and the stronger bond interaction between Cu and S, the VBM from the Cu–S antibonding state is expected to shift up with increasing Cu_{Al} concentration.

In order to investigate the change in VBM position with Cu_{Al} concentration, we have calculated the band offsets among the supercells with different Cu_{Al}^0 concentrations. The band offset was calculated by a commonly used method.[38,39] The average potentials (APs) and the core state eigenvalues of 1s orbital (1s) of host elements far away from defects are chosen as the reference energies. The GGA band-gap error was corrected using a scissor operator. From Fig. 2, one can observe that the VBM shifts up with increasing Cu_{Al} concentration, in line with the results of the analysis of the density of states. According to a recently recognized doping limit rule,[40,41] p-type doping can be fulfilled easily in semiconductor compounds with high VBM, which stands for low formation energy, and a shallow transition level can be realized in the compounds with high VBM. This is the reason for the p-type conductivity in Cu-based compounds, which have high valence positions owing to the high Cu-3d orbital energy. Shifting up the VBM has also been suggested as a remedy to increase the p-type conductivity in the commercialized n-type TCM hosts. For example, in order to increase the p-type conductivity in zinc oxide, some methods aimed to shift up the valence band have been proposed and conducted by different research groups. Through an n- and p-type codoping method,[42] introducing a neutral impurity band above the VBM to shift up the valence band has been used to explain the p-type doping in (Ga+N)-codoped ZnO. Alloying the same valence state elements with higher orbital energy has also been proposed. Since the 3p-orbital energy of sulfur

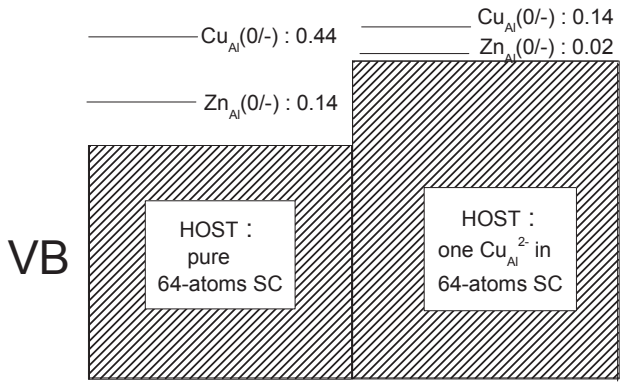

Fig. 3. Calculated acceptor defect levels $\varepsilon(0/-)$ of Cu_{Al} and Zn_{Al} based on two different hosts [i.e., pure $CuAlS_2$ and one Cu_{Al}^{2-} existing in a 64-atom $CuAlS_2$ supercell (SC)].

is higher than the 2p-orbital energy of oxygen, alloying S in ZnO can shift up its valence band[43] and decrease the acceptor transition level, which is suggested to increase its p-type conductivity. Here, we find that heavily doping certain intrinsic defects (i.e., a large composition of a certain component) can also help shift up the valence band and improve the p-type conductivity. Figure 2 shows that the valence band shifts up around 0.3 and 0.6 eV (a consistent result from two different adopted reference energies, i.e., the average potentials and the core state eigenvalues of 1s orbital) after introducing one Cu_{Al}^{0} in 64- and 32-atom supercells, respectively. The change in the original electronic structure may have a marked effect on the defect transition level.

In our earlier works,[19,20] we studied the defect formation energy and transition level by conventional supercell methods.[44,45] In order to overcome the problems from the adopted limited supercells, we have used well-accepted corrections[44,45] to reproduce an unlimited doped supercell, which corresponds to a negligible composition variation of the host. Our calculation suggests that the p-type defect Cu_{Al} has the lowest formation energy and should be the dominant defect under Cu-rich and Al-poor conditions.[20] On the other hand, the acceptor transition level $\varepsilon(0/-)$ of Cu_{Al} is deep and located at 0.44 eV above the VBM,[20] which is consistent with the other calculation results (i.e., 0.44 eV from Ref. 21 and 0.48 eV from Ref. 22). Owing to the deep transition level of Cu_{Al}, our calculated hole concentration is just around $\sim 7.8 \times 10^{16}\,cm^{-3}$ at room temperature under the Cu-rich and Al-poor conditions. From these calculation results, it is difficult to explain the good p-type conductivity (247.5 $S \cdot cm^{-1}$) and large hole concentration ($7.3 \times 10^{19}\,cm^{-3}$) in the $Cu_{1.08}Al_{0.92}S_2$ sample.[14]

When the composition significantly deviates from that of the ideal compounds, we need to calculate the new defect transition level using the modified supercells (i.e., supercells with a large concentration of specific defects). First, we adopted the defect transition levels from our former works.[20] Then, we calculated the change in the defect transition level after one neutral Cu_{Al}^{2-} defect existed in the supercell. Owing to the VBM shifting up because of Cu_{Al}^{2-}, the acceptor transition level $\varepsilon(0/-)$ of another Cu_{Al}^{0} decreases by 0.30 eV and reaches 0.14 eV (Fig. 3). In order to reproduce the hole concentration, we assumed that the charged Cu_{Al}^{2-} defect does not supply and only the neutral Cu_{Al}^{0} defect supplies the hole in the supercell containing two Cu_{Al} defects. Using the Boltzmann distribution law $[c] = N_D \exp[-\varepsilon(0/-)/k_B \cdot T]$ and assuming the effective Cu_{Al}^{0} concentration N_D of $8.3 \times 10^{20}\,cm^{-3}$ (i.e., half of Cu_{Al} in the 64-atom supercell containing two Cu_{Al} defects) and the room temperature T of 300 K, the hole concentration can reach $4.0 \times 10^{18}\,cm^{-3}$, significantly improving the agreement with the experimental result[14] (i.e., hole concentration with $7.3 \times 10^{19}\,cm^{-3}$ in the $Cu_{1.08}Al_{0.92}S_2$ sample). Of note, it is difficult to have the theoretical hole concentration perfectly agree with the experimental value since it is very sensitive to the transition level. If the acceptor transition level $\varepsilon(0/-)$ of Cu_{Al} shifts to 0.06 eV, the experimental hole concentration will be reproduced. Nevertheless, the marked decrease in the acceptor transition level makes us reconsider the defect formation energy and transition level in the samples with a large defect concentration.

From our earlier studies,[20] we learned that the p-type defect Zn_{Al} already has a shallow acceptor transition level, which may further decrease in the Cu-excess samples. The Cu-rich and Al-poor conditions are also suitable for substituting Al by Zn. Zn substituting at the Al site other than the Cu site does not affect the valence band position since Zn at the Al site does not change the electronic state around the VBM, which is largely affected by the amount of Cu. Our calculated acceptor transition level $\varepsilon(0/-)$ of Zn_{Al} decreases by 0.12 eV and reaches 0.02 eV after using the supercell with $\sim$6% Cu_{Al}^{2-}, which means that Zn_{Al} can supply the hole to the host effectively in Cu-excess $CuAlS_2$ samples. Thus, our results suggest that Zn doping at the Al site in Cu-excess $CuAlS_2$ samples is a promising approach to increasing further the p-type conductivity.

In summary, we have investigated the changes in valence band position and defect transition level in Cu-excess $CuAlS_2$ with a large composition variation. The acceptor transition level $\varepsilon(0/-)$ of Cu_{Al} decreases owing to the shifting up of the valence band position in Cu-excess $CuAlS_2$. Our calculated results can qualitatively explain the high p-type conductivity in $Cu_{1.08}Al_{0.92}S_2$. Owing to the shallow acceptor transition level $\varepsilon(0/-)$ of Zn_{Al} in the samples containing $\sim$6% Cu_{Al}^{2-}, our results suggest that Zn substituting at the Al site in Cu-excess $CuAlS_2$ is a promising approach to improving the p-type conductivity.

Acknowledgments This work was financially supported by the National Natural Science Foundation of China (Grant Nos. 61204104, 51271061, 51571065, 61475045, and 11465003), the Natural Science Foundation of Guangxi Province (Grant Nos. 2014GXNSFCA118002 and 2013GXNSFGA019007), and the Scientific Research Foundation of Guangxi University (Grant No. XGZ130718).

1) H. Hosono, Thin Solid Films **515**, 6000 (2007).
2) R. G. Gordon, MRS Bull. **25** [8], 52 (2000).
3) C. G. Granqvist and A. Hultåker, Thin Solid Films **411**, 1 (2002).
4) E. Elangovan and K. Ramamurthi, J. Optoelectron. Adv. Mater. **5**, 45 (2003).
5) H. Agura, A. Suzuki, T. Matsushita, T. Aoki, and M. Okuda, Thin Solid Films **445**, 263 (2003).
6) K. Ellmer, Nat. Photonics **6**, 809 (2012).
7) K. G. Godinho, J. J. Carey, B. J. Morgan, D. O. Scanlon, and G. W. Watson, J. Mater. Chem. **20**, 1086 (2010).
8) G. Thomas, Nature **389**, 907 (1997).
9) D. O. Scanlon and G. W. Watson, J. Mater. Chem. **22**, 25236 (2012).
10) H. Kawazoe, M. Yasukawa, H. Hyodo, M. Kurita, H. Yanagi, and H.

Hosono, Nature **389**, 939 (1997).
11) M. Snure and A. Tiwari, Appl. Phys. Lett. **91**, 092123 (2007).
12) N. Duan, A. W. Sleight, M. K. Jayaraj, and J. Tate, Appl. Phys. Lett. **77**, 1325 (2000).
13) R. Nagarajan, A. D. Draeseke, A. W. Sleight, and J. Tate, J. Appl. Phys. **89**, 8022 (2001).
14) F. Q. Huang, M. L. Liu, and C. Yang, Sol. Energy Mater. Sol. Cells **95**, 2924 (2011).
15) M. L. Liu, Y. M. Wang, F. Q. Huang, L. D. Chen, and W. D. Wang, Scr. Mater. **57**, 1133 (2007).
16) M. L. Liu, F. Q. Huang, and L. D. Chen, Scr. Mater. **58**, 1002 (2008).
17) M. L. Liu, F. Q. Huang, L. D. Chen, Y. M. Wang, Y. H. Wang, G. F. Li, and Q. Zhang, Appl. Phys. Lett. **90**, 072109 (2007).
18) M. Yang, Y. H. Wang, G. F. Li, Z. Shi, and Q. Zhang, J. Vac. Sci. Technol. A **27**, 1316 (2009).
19) D. Huang, Y. J. Zhao, R. Y. Tian, D. H. Chen, J. J. Nie, X. H. Cai, and C. M. Cai, J. Appl. Phys. **109**, 113714 (2011).
20) D. Huang, R. Y. Tian, Y. J. Zhao, J. J. Nie, X. H. Cai, and C. M. Yao, J. Phys. D **43**, 395405 (2010).
21) L. Duclaux, F. Donsanti, J. Vidal, M. Bouttemy, N. Schneider, and N. Naghavi, Thin Solid Films **594**, 232 (2015).
22) L. M. Liborio, C. L. Bailey, G. Mallia, S. Tomić, and N. M. Harrison, J. Appl. Phys. **109**, 023519 (2011).
23) Y. Tani, K. Sato, and H. Katayama-Yoshida, Appl. Phys. Express **4**, 021201 (2011).
24) Y. Wang, M. Liu, F. Huang, L. Chen, H. Li, X. Lin, W. Wang, and Y. Xia, Chem. Mater. **19**, 3102 (2007).
25) S. Park, D. A. Keszler, M. M. Valencia, R. L. Hoffman, J. P. Bender, and J. F. Wager, Appl. Phys. Lett. **80**, 4393 (2002).
26) G. Kresse and J. Hafner, Phys. Rev. B **47**, 558 (1993).
27) G. Kresse and J. Furthmüller, Phys. Rev. B **54**, 11169 (1996).
28) J. P. Perdew, K. Burke, and M. Ernzerhof, Phys. Rev. Lett. **77**, 3865 (1996).
29) D. O. Scanlon, K. G. Godinho, B. J. Morgan, and G. W. Watson, J. Chem. Phys. **132**, 024707 (2010).
30) A. Schleife, C. Rödl, F. Fuchs, J. Furthmüller, and F. Bechstedt, Phys. Rev. B **80**, 035112 (2009).
31) G. Kresse and J. Joubert, Phys. Rev. B **59**, 1758 (1999).
32) H. J. Monkhorst and J. D. Pack, Phys. Rev. B **13**, 5188 (1976).
33) G. Brandt, A. Rauber, and J. Schneider, Solid State Commun. **12**, 481 (1973).
34) W. Zalewski, R. Bacewicz, J. Antonowicz, S. Schorr, C. Streeck, and B. Korzun, Phys. Status Solidi A **205**, 2428 (2008).
35) S. Chen, X. G. Gong, and S. H. Wei, Phys. Rev. B **75**, 205209 (2007).
36) C. Stephan, S. Schorr, M. Tovar, and H. W. Schock, Appl. Phys. Lett. **98**, 091906 (2011).
37) D. Huang and C. Persson, J. Phys.: Condens. Matter **24**, 455503 (2012).
38) W. J. Yin, H. Tang, S. H. Wei, M. M. Al-Jassim, J. Turner, and Y. Yan, Phys. Rev. B **82**, 045106 (2010).
39) Y. Gai, J. Li, S. S. Li, J. B. Xia, and S. H. Wei, Phys. Rev. Lett. **102**, 036402 (2009).
40) S. B. Zhang, S. H. Wei, and A. Zunger, J. Appl. Phys. **83**, 3192 (1998).
41) S. B. Zhang, S. H. Wei, and A. Zunger, Phys. Rev. Lett. **84**, 1232 (2000).
42) Y. Yan, J. Li, S. H. Wei, and M. M. Al-Jassim, Phys. Rev. Lett. **98**, 135506 (2007).
43) C. Persson, C. Platzer-Björkman, J. Malmström, T. Törndahl, and M. Edoff, Phys. Rev. Lett. **97**, 146403 (2006).
44) C. Persson, Y. J. Zhao, S. Lany, and A. Zunger, Phys. Rev. B **72**, 035211 (2005).
45) S. Lany and A. Zunger, Phys. Rev. B **78**, 235104 (2008).